The Complex Formation of Zinc(II) with GHL* and Related Peptides

M. J. A. RAINER and B. M. RODE

Institute of Inorganic and Analytical Chemistry, University of Innsbruck, A - 6020 Innrain 52a, Innsbruck, Austria

Received May 4, 1984

Abstract

The formation constants for complexes of Zn(II) with GHL and related peptides have been determined by means of potentiometric titration and ^{1}H NMR spectroscopy in aqueous solution. GHL has a high affinity for Zn(II) but this somewhat higher affinity compared to the related peptides AH, LH and HL* is not a sufficient explanation for its biological role.

^{1}H NMR spectroscopy allows structural assignment of the relative chemical shifts to complex structures and the method, therefore, is a powerful tool for the determination of complex structures when the metal ion is diamagnetic and the ESR method previously applied to the GHL–Cu(II) system (see ref. 4) cannot be used.

Introduction

GHL is isolated from human plasma in amounts of about 200 ng/cm^3 [1, 2]. In combination with the transition metals copper(II), iron(II) and zinc(II), GHL enhances the growth of cultured hepatoma cells, whereas the addition of these metals without GHL decreases the number of these cells [3]. It is assumed that these metals bind to the membrane where they seem to have toxic effects [3]. Pickart and Thaler [3] postulated a mechanism for the mode of action of GHL: GHL should be able to loosen the connection of the toxic metal ions to the membrane and transport the metals. This hypothesis is supported by our investigations on the Cu(II)–GHL–HSA* system [4].

Besides that, GHL has many other biological functions [5–14]. Many investigations have been carried out which show the biological importance and mechanism of action of GHL (recently reviewed by Pickart [15]). It is known that GHL-related peptides display no biological effects or only low activities [5].

In order to find out the specific properties of GHL in complex formation, which may be responsible for its biological role, in this work the complex formation of GHL with Zn(II) is compared to that with related peptides.

The system Zn(II)–GHL has been investigated so far by ^{1}H NMR spectroscopy only with respect to the location of the binding sites for Zn(II) and Cu(II) at pD = 7.1 [16]. In our work ^{1}H NMR spectroscopy was used to determine formation constants, the spectra of the species and the binding sites appearing at different pD.

The following dipeptides related to GHL were used: HL (the C-terminal dipeptide of GHL), AH and LH representing the N-terminal dipeptide and GL* and VL* in order to determine the influence of lysine as compared to other aliphatic dipeptides like glycylglycine.

Experimental

Materials

$Zn(NO_3)_2 \cdot H_2O$ (analytical grade) was obtained from Merck. The concentration of the Zn(II) stock solution was determined by complexometric titration. All peptides listed in Table I were obtained from Serva and were used without further purification. All aqueous solutions were prepared using CO_2 free distilled water; the ionic strength was 0.1 M $NaNO_3$ in H_2O. Acid and base were Titrisol products (Merck). D_2O (99.80%) was obtained from Stohler Isotope Chemicals.

Potentiometric Titrations

Titrations were carried out at various metal/ligand ratios ranging from 1:1 to 1:4. The Zn(II) concentration was 0.001–0.0025 M. The systems were titrated with 0.4 M NaOH at 37 °C ± 0.3 °C using a 0.2 cm^3 burette (Gilmont) after adding an appropriate amount of HCl.

^{1}H NMR Experiments

The chemical shifts of the protons of the peptides were measured with and without the presence

*Abbreviations: AH = L-histidine-N^2-L-alanyl; GH = L-histidine-N^2-glycyl; GHL = L-lysine-N^2-(-N-glycyl-L-hystidyl); GL = L-lysine-N^2-glycyl; HL = L-lysine-N^2-L-histidyl; HSA = human serum albumin, LH = L-histidine-N^2-L-leucyl; VL = L-lysine-N^2-L-valyl.

0020-1693/84/$3.00

of various amounts of Zn(II) as a function of pD. The concentration of the peptides in solution was kept at 0.1 M in D_2O (99.80%). The metal/ligand ratio ranged from 1:1 to 1:3.33. Chemical shifts are reported relative to the resonance signal of tert. butanol as internal standard. The pD was adjusted with concentrated NaOD and HCl, so that the effect of dilution could be neglected. The spectra were recorded at 32 °C without ionic background. The values for pD were not corrected to pH although the calibration procedure was the same as in the potentiometric titration experiments.

Apparatus

For the pH and pD measurements a Schott pH-meter CG 803 and an Ingold electrode calibrated with standard buffer solutions (Merck) were used. The ^1H NMR spectra were recorded on a Varian EM-360-L 60 MHz spectrometer with a sweep width of 5 or 10 ppm and a sweep time of 5 minutes.

Calculations

All calculations were carried out at the CDC Cyber 74 computer of the University of Innsbruck. 20–30 points per titration and 15–20 ^1H NMR spectra per solution were included in the data representation.

Methods

The method of evaluating the formation constants of complexes from titration curves has been described earlier [17]. For the evaluation of the formation constants and the spectra of the pure species present in the solutions from the ^1H NMR data a new Fortran program (NMROPT) was written. The principles of this program are as follows. Given a solution of a ligand L, containing J different species of the composition $M_pH_qL_r$ from the general reaction:

$$pM + qH + rL \rightleftharpoons M_pH_qL_r \tag{1}$$

where M stands for metal ion and H for proton, each species $M_pH_qL_r$ displays its own ^1H NMR spectrum. If there is a rapid exchange between different species we observe only one signal S_{ik} for the mixture of the J species for each proton i according to eqn. 2:

$$S_{ik} = \sum_{j=1}^{J} f_{ij} X_{jk} \tag{2}$$

$1 \leqslant i \leqslant I$ kind of proton
$1 \leqslant j \leqslant J$ kind of species present in the solution
$1 \leqslant k \leqslant K$ index for the number of experimental measurement points
X_{jk} molar fraction of species j at point k times r_j
f_{ij} chemical shift of proton i in species j

We can obtain X_{jk} for any given set of reactions (eqn. 3) and its formation constants pK_{pqr} by the application of the Newton method [18]

$$pK_{pqr} = -\lg\left(\frac{M_pH_qL_r}{m^p h^q l^r}\right) \tag{3}$$

if p, q and r are the stoichiometric quantities of M, H and L and m, h and l are the concentrations of free M, H and L respectively.

The calculation starts with an arbitrary set of pK_{pqr} and f_{ij} ($j \neq \bar{j}$) ($\bar{j}$ being the species number for which we want to calculate its $f_{i\bar{j}}$ and $pK_{\bar{p}\bar{q}\bar{r}}$).

For a given set of pK_{pqr}, $f_{i\bar{j}}$ can be calculated from eqn. 4 for all i:

$$f_{i\bar{j}} = \frac{\sum_{k=1}^{K} X_{\bar{j}k}\left(S_{ik}^{exp} - \sum_{j\neq\bar{j}}^{J} f_{ij} X_{jk}\right)}{\sum_{k=1}^{K} X_{\bar{j}k}^2} \tag{4}$$

$f_{i\bar{j}}$ are the values which lead to the lowest F (see eqn. 5) within a given set of pK_{pqr} and f_{ij} ($j \neq \bar{j}$). Only those k where $X_{\bar{j}k}$ was higher than 0.02 were taken into account. After that $pK_{\bar{p}\bar{q}\bar{r}}$ is varied systematically, each variation leading to a new $f_{i\bar{j}}$. The combination of $f_{i\bar{j}}$ and $pK_{\bar{p}\bar{q}\bar{r}}$ which leads to the lowest F (see eqn. 5) is chosen for the next steps.

$$F = \sum_{k=1}^{K}\sum_{i=1}^{L}(S_{ik}^{exp} - S_{ik}^{calc})^2 \longrightarrow F_{min} \tag{5}$$

In the next steps we choose other species for $\bar{j}$ and repeat the procedure in a cyclic manner until the error function F converges to a minimum F_{min}. Thus the best set of f_{ij} and pK_{pqr} is obtained.

If the quality of the simulation is poor, one has to change or enlarge the chemical model underlying the procedure.

Interpretation of the Spectra

Only those ^1H NMR signals were taken into account which could be assigned reliably to specific protons of the ligands. Under the given experimental conditions (water content of the peptides and of $Zn(NO_3)_2$; D_2O of 99.80% purity; 60 MHz spectra) this assignment was not possible with the desired accuracy for those nuclei not mentioned in Table II.

GHL Spectra

The signals of the imidazole protons 1 and 2 (notation Fig. 5) show a doublet (J = 1.5 Hz) and appear

as broad singlets at higher pD and in the case of complex formation with zinc(II) [16]. The diastereotopic protons of glycine should give rise to an AB system (a doublet for each proton; J = 16 Hz; [16]), but appear as triplets over the whole pD range. The β-methylene protons of histidine appear as a doublet (J = 7 Hz) and the ε-methylene protons display a distorted triplet (J = 7.2 Hz).

AH Spectra

The methyl protons of alanine show a doublet (J = 7.2 Hz) and the α-proton of alanine displays a quadruplet (J = 7.2 Hz). The β-methylene protons of histidine show a distorted doublet (J = 6.6 Hz) as in the case of GHL but we observe a splitting of the doublet in solutions with pD higher than 7.6. This may be due to the change in the spin system AX_2 to ABC as has been reported for pure histidine [19]. Therefore this signal was not taken into account for solutions with pD higher than 7.6. Imidazole protons are observed as in the case of GHL.

GL Spectra

The methylene protons of glycine display a singlet. Due to long range coupling both the α- and ε-methylene protons show distorted triplets over the whole pD range, both having a coupling constant of J = 7 Hz.

Results

Table I displays the pK_{pqr} values for the pure ligands L (p = 0), where L denotes the anion in all

TABLE I. Protonation and Complex Formation Constants.

p	q	r	GHL				
			pot. titr.		^{1}H NMR		literature
			pK_{pqr}	dpK_{pqr} [a]	pK_{pqr}	dpK_{pqr} [b]	
0	4	1	−26.51 [c]	0.19	n.d. [d]	n.d. [d]	−27.81 [e], −27.72 [f]
0	3	1	−23.99 [c]	0.09	−24.35	0.13	−24.90 [e], −24.63 [f], −25.37 [g]
0	2	1	−17.66 [c]	0.10	−17.79	0.17	−18 37 [e], −18.18 [f], −18.77 [g]
0	1	1	−10.01 [c]	0.20	−10.05	0.24	−10.44 [e], −10.34 [f], −10.71 [g]
1	2	1	n.d. [d]	n.d. [d]	−20.03	0.26	
1	0	1	−7.50	0.06	−7.76	0.75	

p	q	r	AH					LH	
			pot. titr.		^{1}H NMR		literature	pot. titr.	
			pK_{pqr}	dpK_{pqr} [a]	pK_{pqr}	dpK_{pqr} [b]		pK_{pqr}	dpK_{pqr} [a]
0	3	1	−16.81	0.13	−17.11	0.42	−17.53 [f]	−16.52	0 15
0	2	1	−14.29	0.05	−14.48	0.15	−14.71 [f]	−14 16	0.06
0	1	1	−7.79	0.07	−7.83	0.14	−8.04 [f]	−7.72	0.06
1	1	1	−9.87	0.90	−10.05	0.33		−10.01	0 40
1	−1	1	3.23	0.08	2 80	0.80		3.28	0.08
1	1	2	n.d. [d]	n.d. [d]	−14.00	0.60		−13.65	0.85

p	q	r	GL				VL		HL		
			pot. titr.		^{1}H NMR		pot. titr.		pot. titr.		literature
			pK_{pqr}	dpK_{pqr} [a]	pK_{pqr}	dpK_{pqr} [b]	pK_{pqr}	dpK_{pqr} [a]	pK_{pqr}	dpK_{pqr} [a]	
0	4	1							−25.05	0.29	−26.18 [f]
0	3	1	−20.54	0.24	−21.42	0.22	−20.56	0.16	−23.03	0.08	−23.57 [f]
0	2	1	−17.78	0.12	−18.57	0.15	−17.47	0.05	−17.38	0.07	−17.72 [f]
0	1	1	−10.01	0.15	−10.40	0 28	−10.00	0.07	−10.09	0.09	−10.35 [f]
1	1	1	−13.16	0.20	−13 39	0 26	−12.01	0.75	−14.78	0.11	
1	2	2	−26.12	0.22	−26.23	0.65	−24.94	0.80	−28.60	0.16	

[a] If pK_{pqr} is varied by $\pm dpK_{pqr}$, the experimental error $(\Sigma_{k=1}^{K} (base_{added}^{calcd.} - base_{added}^{exper.})^2$ is doubled [b] If pK_{pqr} is varied by $\pm dpK_{pqr}$, the experimental error F (see eqn 5) is doubled [c] See also ref. [4] [d] n.d.: not detectable by this method. [e] Potentiometric titration, 25 °C, 0.15 M NaCl; see ref [20]. [f] ^{1}H NMR, 37 °C, D_2O, see ref [21] [g] ^{1}H NMR, 25 °C, 0.08 M KCl, see ref. [22].

TABLE II. Calculated Chemical Shifts (ppm to t-BuOH).

			GHL					AH					GL		
p	q	r	1[a]	2[a]	3[a]	4[a]	5[a]	1[b]	2[b]	3[b]	4[b]	5[b]	1[c]	2[c]	3[c]
0	3	1	7.31	6.05	2.58	2.00	1.75	7.36	6.08	2.82	2.07	0.28	3.15	2.60	1.74
0	2	1	6.61	5.77	2.58	1.86	1.74	7.31	5.98	2.78	1.94	0.27	2.90	2.57	1.73
0	1	1	6.35	5.63	2.18	1.79	1 75	6.52	5.68	2.82	1.81	0.31	2.89	2.08	1.74
0	0	1	6.37	5.65	2.05	1.80	1.29	6.37	5.63	2.26	1 78	−0.03	2.88	2 06	1.27
1	2	1	6.41	5.66	2.53	1.90	1.74								
1	1	1						6.38	5.51	2.79	1.87	0.26	2.92	2.25	1.74
1	0	1	6.58	5.70	2.35	1.88	1.73								
1	−1	1						6.42	5.08	2.43	1.70	−0.08			
1	1	2						6.57	5.68	2.69	1.86	0.16			
1	2	2											2.86	2.29	1.74

[a]See Fig. 5. [b]See Fig. 6. [c]See Fig 8

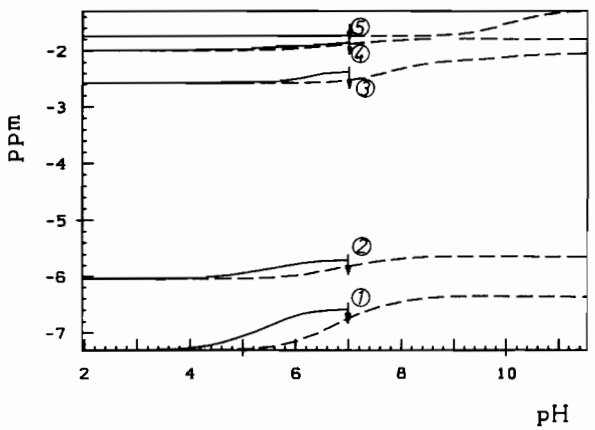

Fig. 1. Calculated ^{1}H NMR titration curves· – – – 0.1 M GHL; —— 0 1 M GHL + 0 1 M Zn(II); ↓ precipitation; ⓝ notation for the kind of proton (see Table II and Fig. 5)

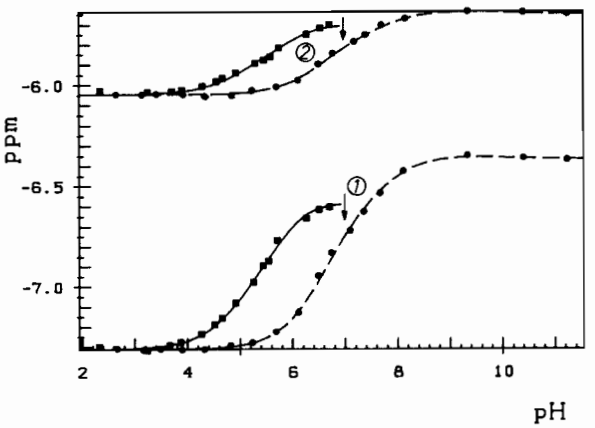

Fig. 2. Calculated and experimental ^{1}H NMR titration curves for the imidazole protons 0 1 M GHL – – – calculated, • experimental. 0.1 M GHL + 0.1 M Zn(II)· —— calculated, ▪ experimental.

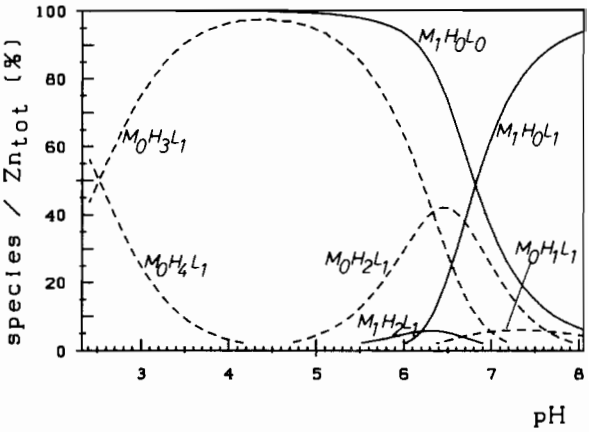

Fig. 3. Distribution of species as a function of pH. 0.001 M GHL + 0 001 M Zn(II); pK_{pqr} taken from potentiometric titration; pK_{121} taken from ^{1}H NMR experiments.

cases. The pK_{pqr} values obtained by the two different methods overlap within their standard deviations, although the conditions differed in temperature, solvent, concentration and ionic background. The largest difference was found in the case of GL. Table I also lists the 'best' sets of pK_{pqr} with p ⩾ 1 for both methods. Table II displays the calculated chemical proton shifts of the pure species $M_pH_qL_r$. Figures 1 and 2 show the '^{1}H NMR titration curves' for pure GHL and GHL–Zn(II) (1·1) as examples of the high quality of the simulation. Due to the very low concentration in the potentiometric titrations as compared to that of the ^{1}H NMR solutions we could not determine some of the constants with the former method, because the concentrations of these complexes are negligible in the case of very low concentrations (noted by n.d. in Table I). A very interesting example is the complex $M_1H_2L_1$ in the case of GHL and the complex $M_1H_1L_1$ in the case of AH. This kind of complex (see Discussion) shows a very low stability and hardly improves the quality of the

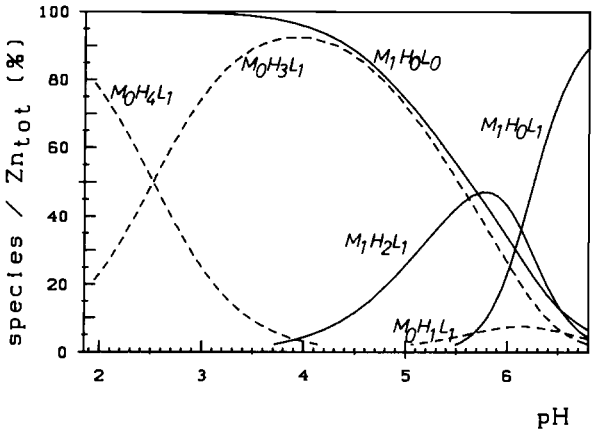

Fig. 4. Distribution of species as a function of pH: 0.1 M GHL + 0.1 M Zn(II); pK_{pqr} from ^{1}H NMR experiments.

simulation in the potentiometric titration experiments. At the higher concentrations present in the ^{1}H NMR experiments, however, this complex can bind relatively large amounts of zinc(II) and is necessary therefore for the simulation based on ^{1}H NMR data. In any case if we apply the model obtained by the ^{1}H NMR method to the conditions of the potentiometric titrations, we obtain negligible concentrations for all species which could not be determined by the potentiometric method (see Figs. 3 and 4).

Discussion

Before discussing the different complex formation behaviour of the ligands some general rules for the interpretation of the spectra should be adopted.

1) The replacement of a proton by Zn(II) leads to a sharp upfield shift for protons near the center of the replacement (see also refs. [17, 23]).

2) The total loss of a proton from aliphatic nitrogens will cause a larger upfield shift than its replacement by Zn(II) [17, 23], so that a general complex $M_aH_bL_c$ will display a downfield shift for protons near the complex binding site, compared to the pure species $M_0H_bL_c$.

3) The extent of the shift depends on the number of bonds located between proton and complex binding site. The deshielding effect of Zn(II) or protons as mentioned in 2) is higher for protons separated by even bond numbers than for those separated by odd bond numbers [24] and the effect may even be reversed in the latter case.

Rule 2 could only be verified for aliphatic parts of the ligand, especially for the N-terminal amino end structure, whereas the aromatic system reacts in a more complicated way on complex formation.

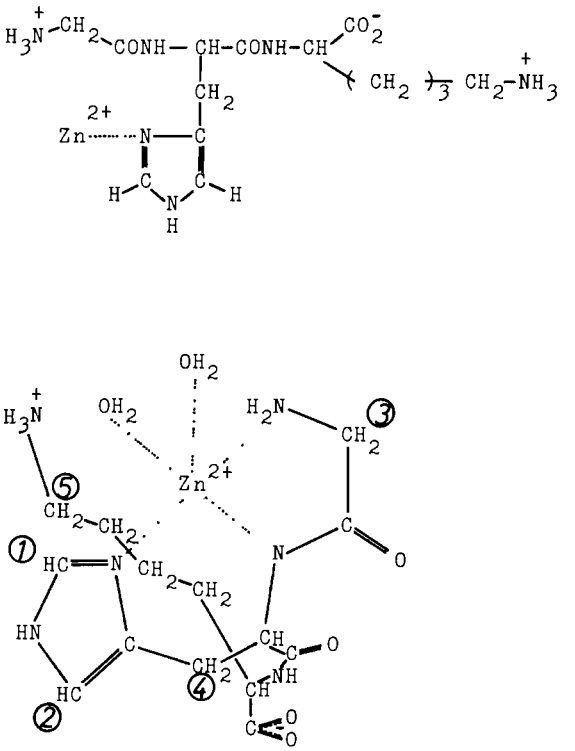

Fig. 5. Proposed structure for the GHL–Zn(II) complexes: ⓝ notation for the kind of proton (corresponding to Table II).

One can deduce from Table I that the ligands can be divided into three types with different complex formation behaviour.

L = GHL. As mentioned above, the complex $M_1H_2L_1$ could only be detected in reasonable amounts in the ^{1}H NMR experiments and has a very low stability. When this complex is formed from $M_0H_3L_1$ the only remarkable relative shifts (see rule 1) are observed for the imidazole ring protons. Therefore this complex should be a unidentate complex with imidazole nitrogen (Fig. 5).

It is interesting that we could not detect a $M_1H_1L_1$ complex by both methods. Figure 5 gives a possible explanation: the structure element GH* (together with the side chain of lysine) is capable of 'embedding' ions very closely, so that GHL prefers to release two protons at once to chelate Zn(II). The complex $M_1H_0L_1$ is the only complex found in the potentiometric titration experiments. It is a very stable complex with a tridentate structure (Fig. 5). Although the side chain of lysine contributes to the high stability (see conclusion), the ϵ-amino group of lysine is not involved in complex formation as we can deduce from the fact that the signal of the ϵ-methylene protons is not shifted. This is in good agreement with the work of Kwa *et al.* [16] and our work on the Cu(II)–GHL system [4]. The complex $M_1H_0L_1$ therefore has a proto-

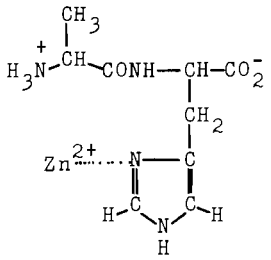

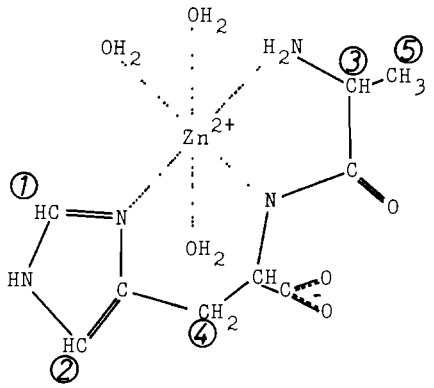

Fig. 6. Proposed structures for the 1 1 AH–Zn(II) complexes. ⓝ notation for the kind of proton (corresponding to Table II)

nated ϵ-ammonium group; the proton is released from the peptide bond.

According to rule 2 we find a downfield shift for the glycyl methylene protons in $M_1H_0L_1$ as compared to $M_0H_1L_1$ (free amino group). GHL forms no complexes with the composition $M_aH_bL_c$, $a \geqslant 1$, $c > 1$.

L = AH, LH. The complex $M_1H_1L_1$ could be detected by both methods (but with high standard deviation dpK_{111} in the potentiometric titrations) and has the same structure and almost the same stability as the corresponding complex for GHL ($M_1H_2L_1$); besides, the relative chemical shifts are the same so that we can again propose a unidentate structure (see Fig. 6). As in the corresponding complex of GHL, AH and LH prefer to release two protons simultaneously from $M_1H_1L_1$ forming $M_1H_{-1}L_1$. The relative chemical shifts are nearly the same as in the case of GHL, with the exception of the imidazole proton 2 (see Table II). The proposed structure is shown in Fig. 6 and corresponds to that of the GHL–Zn(II) complex. AH and LH are able to form low stability 1:2 complexes of the composition $M_1H_1L_2$.

L = GL, VL, HL. These ligands formally display the same model description for the complex formation with Zn(II). Zn(II) is not able to detach the proton from the peptide nitrogen. The ligands form

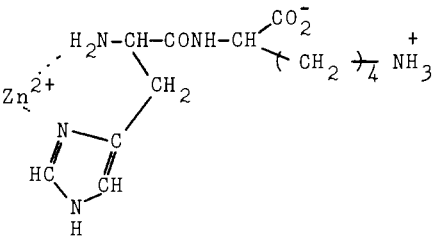

Fig. 7. Proposed structure for the $M_1H_1L_1$ complex of HL with Zn(II).

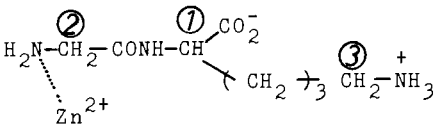

Fig. 8 Proposed structure for the $M_1H_1L_1$ complex of GL with Zn(II) ⓝ notation for the kind of proton (corresponding to Table II).

$M_1H_1L_1$ complexes and the corresponding 1:2 complexes $M_1H_2L_2$. The stability of the complexes decreases from HL to GL to VL. The complexes with Zn(II)–HL are more stable than that with GL because Zn(II) is bound by the amino end and the imidazole nitrogen, (Fig. 7) whereas GL binds Zn(II) with its amino end and only a weak binding to the peptide group (Fig. 8) takes place [25]; therefore only the protons of the glycyl methylene group are shifted considerably upfield as compared to $M_0H_2L_1$ (rule 1) and shifted downfield as compared to $M_0H_1L_1$ (rule 2). The ϵ-amino group of lysine remains protonated when Zn(II) is bound (unshifted ϵ-methylene protons as in the case of GHL). As we know from former work [17, 25] the stability of the $M_1H_1L_1$ complex increases with the basicity of the amino end nitrogen and decreases with the size of the side chain of the N-terminal amino acid (steric hindrance).

In comparison with GL, VL has lower basicity of the amino end nitrogen and a very bulky side chain. This must be the reason for the very low complex stabilities in the case of VL. The lysine residue at the C-terminal position seems to have no direct influence on the complex formation constants with Zn(II). for instance, GL displays the same model as glycylglycine [25], the stabilities of the complexes are almost the same.

Conclusion

As pointed out in our previous communication [4] we cannot compare the formation constants of complexes if the ligands differ in their protonation behaviour. In order to compare the relative affinities of GHL and its related peptides to Zn(II),

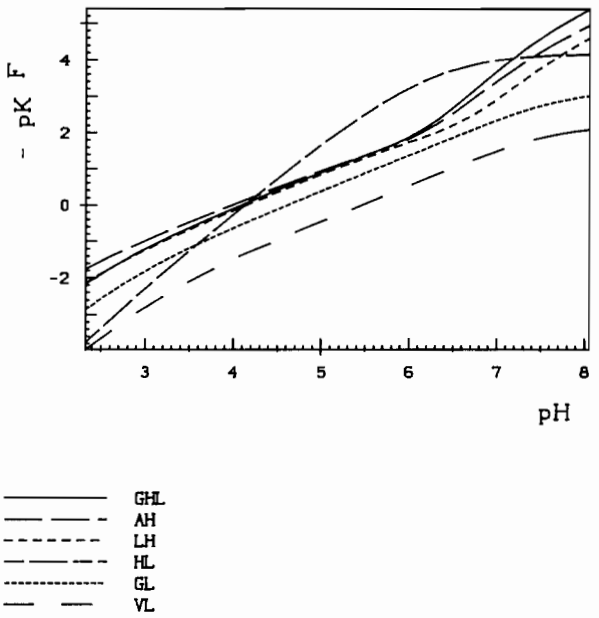

Fig. 9. pK^F as a function of pH: pK_{pqr} taken from potentiometric titration $M \cdot L \cdot L^F = 1:1:1$.

one can compare the pK^F as a function of pH. pK^F is defined as the complex formation constant for a complex of M with a fictive ligand L^F ($M + L^F \rightleftharpoons ML^F$) which would bind M to the same extent as the real ligand L in all complexes M_pH_q-L_r ($p \geqslant 1$) together. This diagram is shown in Fig. 9. At physiological pH = 7.4 GHL has the highest affinity to Zn(II), followed by AH, HL and LH and further GL and VL. The specific properties of GHL in complex formation seem to be therefore (see also refs. [4, 16, 26]):

a) The presence of the structure element GH which is able to split a proton from the peptide nitrogen when Zn(II) is bound. This functionality is also present in AH and LH; but Zn(II) cannot split off this proton in HL, GL and VL.

b) Although the ϵ-amino group of lysine is not involved in complex formation, the side chain of lysine may cause an additional 'embedding effect', which leads to a somewhat higher affinity for Zn(II) as compared to AH and LH, and which may be the reason that GHL does not form 1:2 complexes with Zn(II) (steric hindrance).

c) The higher affinity for Zn(II) cannot be a satisfactory explanation for the biological functions of GHL; in addition the ϵ-amino group of lysine should act as a further functional element, most probably in its protonated form, which could allow donor–acceptor interaction with the other molecules involved [3, 4, 26].

References

1 L. Pickart and M. M. Thaler, *Nature New Biol., 243,* 85 (1973).
2 L. Pickart and M. M. Thaler, *J. Chromatography, 175,* 65 (1979).
3 L. Pickart and M. M. Thaler, *J. Cell. Physiol., 102,* 129 (1980).
4 M. J. A Rainer and B. M. Rode, *Inorg. Chim. Acta, 92,* 1 (1984).
5 L. Pickart and M. M. Thaler, *FEBS Lett., 104,* 119 (1979).
6 B. E. Stromberg, P B. Khoury and E. J L. Soulby, *Int J. Parasit., 7,* 149 (1977).
7 J. P. Dessaint, D. Camus, E. Fischer and A. Capron, *Eur J. Immun., 7,* 624 (1977).
8 M. Sensenbrenner, G. G. Jaros, G. Moonen and P. Mandel, *Neurobiology, 5,* 207 (1975).
9 M. Capron, A. Capron, G. Torpier, H Bazin, D. Bout and M. Joseph, *Eur. J. Immun., 8,* 127 (1978).
10 K H. Slotta, A. L. Golub and V. Lopez, *Hoppe-Seyler's Z. Physiol. Chem., 356,* 367 (1975).
11 M. Joseph, J. P. Dessaint and A Capron, *Cell Immun., 34,* 247 (1977).
12 L. Holmberg, I. Lecander, B. Persson and B. Astedt, *Biochim. Biophys. Acta, 544,* 128 (1978).
13 M. K. Leung, L. J. Fessler, D. B. Greenbert and J. H. Fessler, *J. Biol. Chem , 254,* 224 (1979)
14 L. Svanberg and B. Astedt, *Experientia, 35,* 818 (1979).
15 L. Pickart, *Lymphokines, 8,* 425 (1983).
16 E. Y. Kwa, B. J. Rose, B. Weinstein and L. Pickart, 8th American Peptide Symposium, in press.
17 M. J. A. Rainer and B. M. Rode, *Inorg. Chim. Acta, 58,* 59 (1982).
18 W S. Kittl and B. M. Rode, *J. Chem. Soc., Dalton Trans , 3,* 409 (1983)
19 R. H. Carlson and Th. L. Brown, *Inorg. Chem , 5* (2), 268 (1966).
20 S. J. Lau and B. Sarkar, *Biochem. J , 199,* 649 (1981).
21 M. Tanokura, M. Tasumi and T. Miyazawa, *Biopolymers, 15,* 393 (1976).
22 D. L. Rabenstein, M. S. Greenberg and Ch. A Evans, *Biochemistry, 16* (5), 977 (1977).
23 M. J. A. Rainer and B. M. Rode, *M Chem., 133,* 399 (1982).
24 V. Gutmann, 'The Donor-Acceptor Approach to Molecular Interactions', New York-London, 1978.
25 W. S. Kittl and B M. Rode, *Inorg. Chim Acta, 63,* 47 (1982).
26 C. M. Perkins, J. R. Rose, R. E. Stenkamp, L. H. Jensen, B. Weinstein and L. Pickart, *Inorg Chim Acta,* in press.